Evaluation of Isolated Three-phase AC-DC Converter using Modular Multilevel Converter Topology

Toshiki Nakanishi
Dept. of Electrical, Electronics and Information Engineering
Nagaoka University of Technology
Nagaoka, Niigata, Japan
nakanishi@stn.nagoakaut.ac.jp

Jun-ichi Itoh
Dept. of Electrical, Electronics and Information Engineering
Nagaoka University of Technology
Nagaoka, Niigata, Japan
itoh@vos.nagaokaut.ac.jp

Abstract— **This paper discusses an isolated three-phase AC-DC converter using Modular Multilevel Converter (MMC) topology for a medium voltage application. The MMC at a primary stage of an isolated AC-DC converter directly obtains the high frequency AC voltage from the three-phase AC voltage of the commercial frequency. In addition, the proposed system obtains the low total harmonic distortion (THD) in the input current and maintains the cell capacitor voltage at constant. The comparative evaluations of the system design based on the rated voltage of switching devices are considered. In particular, the numbers of cells and switching devices, the electrostatic energy of the DC capacitors, the THD of the input current and device losses are evaluated when high rated voltage devices: 2.5-kV IGBTs, 3.3-kV IGBTs and 3.3-kV SiC-MOSFETs are applied to the proposed system.**

Keywords— Modular Multilevel Converter; Capacitor Voltage Control; High Frequency Transformer; H-bridge Cell; Isolated Three-phase AC-DC converter;

I. INTRODUCTION

Recently, a DC distribution network system in datacenters has been actively researched in order to achieve size reduction of the network [1-3]. Moreover, in order to obtain the high efficiency operation, a medium voltage such as 6.6 kV is employed as the power source. In addition, DC voltage of 1 kV or less is supplied to a load such as a server supply by an isolation transformer and a rectifier. However, the conventional system becomes large due to passive components. A diode bridge or a PWM rectifier which is constructed from high rated voltage devices is applied in the conventional system. In general, it is difficult to operate in high switching frequency for a high rated voltage device. Thus, large passive components are required due to low switching frequency in order to suppress harmonic distortion of input current and voltage ripple of output DC voltage.

On the other hand, the multilevel converter is one of effective solution for the problem of above. Recently, the multilevel converter topologies have been actively discussed for the medium voltage application such as at 3.3 kV or 6.6 kV [4-10]. Especially, Modular Multilevel Converter (MMC) has been actively studied as one of the multilevel converter topologies [5]. Advantages of the MMC are as follows; (i) the circuit configuration is simpler than that of other multilevel converters due to cascade connection of cells. Each of the cells is constructed from switching devices and a DC capacitor, (ii) the MMC can reduce the harmonic distortions because the MMC output the multilevel waveform as with other multilevel converters. (iii) low voltage devices can be applied to each cells because the output voltage becomes low by increasing a number of cells. In addition, the MMC achieves the size reduction of passive components due to high frequency operation by low voltage devices. From the advantages of the above, the MMC topology can be applied in high capacity power applications such as Static Synchronous Compensator (STATCOM) and medium range of adjustable speed drive systems [11-15].

However, the high power converters which use MMC result that the volume of the converters becomes large due to the isolation transformer which is operated with line-frequency. The isolation transformer is applied in order to separate the grid side and the load side in order to protect the server supply. One of the effective ways to reduce the transformer size is applying high frequency operation. The size reduction of the transformer by using the multi-module converter has been reported [16-17]. In back-to-back (BTB) systems, multiple bidirectional isolated DC-DC converters are considered and consequently the size reduction of the transformer is achieved due to the usage of the high frequency transformer to each isolated DC-DC converter [9]. However, in principle, it is difficult to achieve high efficiency because the number of switching devices drastically increases with increasing the number of stages. Moreover, a DC-DC converter which has high frequency AC link using MMC has been proposed [18]. In the BTB system, the size reduction of the transformer can be achieved because the transformer is used in high frequency AC link [10]. However, the number of cells is

large because MMC has to be applied to both the input and the output sides.

This paper discusses an isolated three-phase AC-DC converter using MMC and a control strategy. Three-phase to single-phase MMC topology is used at a primary stage in the isolated AC-DC converter. The proposed system directly converts three-phase voltage into high frequency single-phase voltage. Furthermore, the volume of the proposed system becomes small and simple due to a high frequency single-phase transformer.. It is confirmed by the simulation that the proposed system achieves low THD and the cell capacitor voltage remains at constant. In addition, the comparative evaluations of the system design based on the rated voltage of switching devices are considered. In particular, the numbers of cells and switching devices, the electrostatic energy of the DC capacitors, the THD of the input current and the device losses are evaluated when high rated voltage devices: 2.5-kV IGBTs, 3.3-kV IGBTs and 3.3-kV SiC-MOSFETs are applied into the proposed system.

II. Main Circuit Configuration

Fig. 1(a) shows the circuit configuration of the isolated three-phase AC-DC converter using MMC topology. Due to the cascade connection of cells, the proposed converter can achieve a multilevel voltage waveform and the rated voltage of each cell is reduced as well. Thus, increasing the number of cascaded cells are effective because the harmonic distortions of an input current can be reduced, and low voltage rating switching devices can be used.

Furthermore, the proposed system can directly convert an input three-phase voltage into a high frequency single-phase voltage. Therefore, the volume of the proposed system becomes small due to the use of the high frequency transformer. In addition, the topology is symmetry from input and output side. Thus, the proposed system can control each of group independently. In this paper, the group in the upper side is defined as an arm group A, and the group in the lower side is defined as an arm group B.

Fig. 1(b) shows the configuration of an H-bridge cell. The output voltage of each cell is controlled by pulse width modulation (PWM). Moreover, it is necessary to ensure the capacitor voltage at constant for a stable operation of the main circuit.

III. Control Strategy

Fig. 2 shows the control block diagram of the proposed converter. The proposed control is applied to each group A and B, respectively as shown in Fig. 1. The proposed control block diagram is separated into two blocks, the capacitor voltage control block and the input current control block. Moreover, two types of control are used in the capacitor voltage control block, an average control and a balance control [19].

A. Average Voltage Control

The average voltage control corrects the error between the average value of the capacitors voltage in each arm group and the voltage command is generated from a PI regulator. The average value of the capacitor voltage v_{c_ave} is given by (1)

$$v_{c\_ave} = \frac{2}{3n}\sum_{m=1}^{n/2}\left(v_{crm} + v_{csm} + v_{ctm}\right) \tag{1}$$

where n is the number of cells in each leg and v_{crm}, v_{csm} and v_{ctm} are the capacitor voltage in the each arm. The number of cells is set $n/2$ in order to calculate the average value of the capacitors voltage in each arm group because each arm group is independently controlled.

B. Balance Voltage Control

The average voltage control is used to keep the voltage of all capacitors at constant level. However, an unbalance voltage which occurs among the capacitors cannot be suppressed by the average voltage control because the average control only corrects the error between the average value of the capacitors voltage in each group and subjects to the voltage command. Therefore, the balance voltage control is used in order to correct the error between each of the capacitors voltage and the voltage

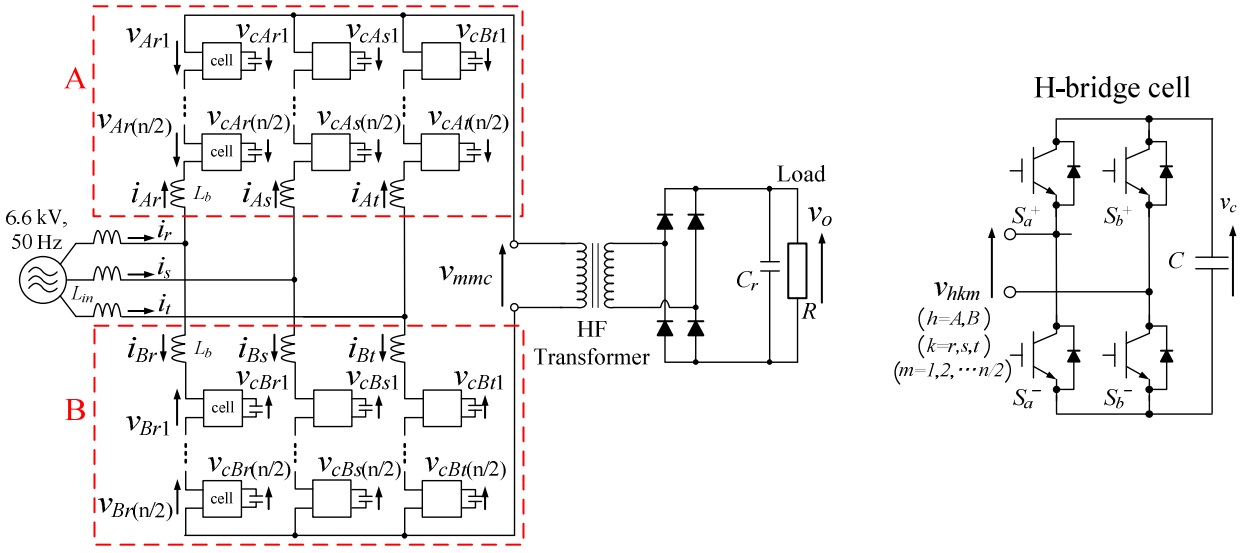

(a) Main circuit configuration.

(b) H-bridge cell.

command. The command of the balance control is given by (2)

$$v_{ce\_Akm}{}^{*} = K_C\left(v_c{}^{*} - v_{c\_km}\right) i_k \tag{2}$$

$$k = r,s,t \quad m = 1,2,\ldots n/2$$

where v_{crm}, v_{csm} and v_{ctm} are the capacitor voltage in each arm respectively, K_C is the gain of the balance voltage control, k is the index of each phase and m is the index of number of cells.

Moreover, it is not necessary to eliminate the error completely because the balance control is an auxiliary control for the average voltage control. Therefore, the balance control can be constructed only by using proportional control.

C. Input Current Control

The input current flows separately to the upper side arm and the lower side arm in each phase. Therefore, the input current can be determined by controlling the current which flow into the buffer reactors. In addition, in the input current control, the linkage operation is not needed between the arm group A and B. Furthermore, the proposed system is able to control the arm groups A and B respectively.

The input current control is implemented by PI regulators and the compensators for the cross terms of i_d and i_q which are provided from the transformation of rotating frame. The input current control is separated into the active current control (i_d) and the reactive current control (i_q). The reactive current command $i_q{}^{*}$ is set to zero in order to control the input power factor to 1 and to reduce the absolute value of the input current. Therefore, the same input current command is given to each cell because the cascaded cells control the common arm current.

D. Output Voltage Control

The same command of the MMC output voltage control is given to each cell in order to convert a three-phase input voltage to a high frequency voltage. The output voltage of a cell is $v_{mmc}{}^{*}/n$ when the command of the MMC output voltage control is $v_{mmc}{}^{*}$ and the number of cells in a leg is n.

Finally, the output voltage of the cell is given by (3). Note that the sign of the MMC output voltage command $v_{mmc}{}^{*}$ has to be changed because the direction of cell output voltage is different in the group A and the group B.

$$\begin{aligned} v_{Akm}{}^{*} &= \frac{1}{n}\left(2v_{Ak}{}^{**} + v_{mmc}{}^{*}\right) - v_{ce\_Akm}{}^{*} \\ v_{Bkm}{}^{*} &= \frac{1}{n}\left(2v_{Bk}{}^{**} - v_{mmc}{}^{*}\right) - v_{ce\_Bkm}{}^{*} \end{aligned} \tag{3}$$

$$k = r,s,t \quad m = 1,2,\ldots n/2$$

E. Capacitor Voltage Command

The MMC output voltage command $v_{mmc}{}^{*}$ is added in order to obtain the high frequency output voltage, which is added to the output block of the input current control. The change of voltage values in each cell depends on the number of cells at each leg since the cells are connected to the load in parallel. In addition, each capacitor voltage also depends on the input and output voltage. The capacitor voltages command $v_c{}^{*}$ is given by (4).

$$v_c{}^{*} \geq \frac{1}{n}\left(2\sqrt{\frac{2}{3}}E + v_{mmc}{}^{*}\right) \tag{4}$$

where E is the effective value of the input line to the line voltage, $v_{mmc}{}^{*}$ is the maximum value of the MMC output voltage command and n is the number of cells at each leg. From (4), the capacitor voltage of each cell becomes smaller by increasing the number of cells. Therefore, the capacitor voltage command becomes lower.

IV. Evaluation of the Proposed System

A. Evaluation Condition

Table 1 shows the parameters of the switching devices with the high rated voltage. In the proposed system, from (4), the capacitor voltage depends on the input current control and the MMC output voltage control. Therefore, the rated voltage of the switching devices depends on the capacitor voltage of the cell. In the case where the high rated voltage devices are applied, it is possible to reduce the number of the circuit components in the proposed

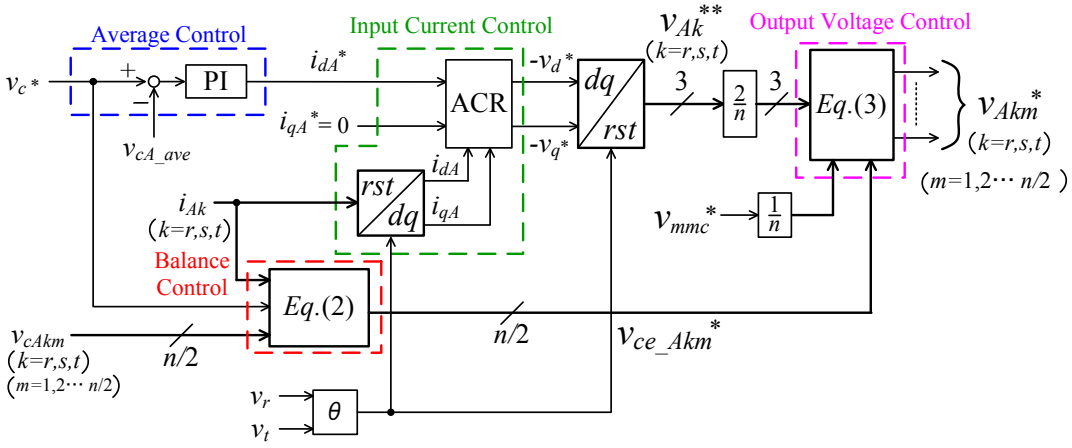

Fig. 2. Control block diagrams of the proposed circuit for the arm group A.

system. On the other hand, in the case where the low rated voltage devices are applied and the number of cells is increased, it is possible to suppress the harmonic distortion of the input current due to the high speed switching and multiple voltage levels. Thus, the design factors : the number of cells, the capacitor voltage and the THD of the input current are different. Therefore, comparing of the circuit performance based on the rated voltage of switching devices is required. In order to compare the circuit performance with different devices, the number of high rated voltage IGBTs and SiC MOSFETs which the rated voltage is 3.3-kV are employed.

The conditions to compare the circuit performance are as follow.

a) The rated voltages of IGBTs are 2.5-kV, 3.3-kV and 6.5-kV, respectively.

b) The capacitor voltage is set 20% more than the value which is calculated by (4). Moreover, the rated voltage is set 30% more than the capacitor voltage.

c) The output power is set at 400 kW and the output voltage is set at 450 V.

d) MMC output voltage command v_{mmc}^{*} is set 2.6 kV, 1 kHz.

e) Buffer reactor L_b is 0.5 mH (the percentage of impeadance $\%Z$ = 0.31%). Moreover, the interconnection reactor is 4 mH (the percentage of impeadance $\%Z$ = 0.125). Both reactors are common value in all system.

f) Switching frequency is chosen so that the proposed system can achieve the efficiency of 95% with considering of the devices loss: the conduction loss, the switching loss and the conduction loss of the free wheeling diode (FWD).

B. Comparative Evaluation of the proposed system

The number of cells, switching devices and DC capacitors are estimated by referring (4) and condition (b) is listed in previous part.

Table 2 shows the comparison result of the cell numbers and switching devices that depends on the rated voltage of the switching device.

In the case where IGBTs with the rated voltage of 2.5-kV are applied, 10 cells are required per leg. Moreover, 120 units of IGBT are required. On the other hand, 2.5-kV IGBT can be set as a high response angular frequency due to high speed switching. Therefore, it is possible to reduce the values of buffer reactors and DC capacitors, respectively.

On the other hand, in the case where IGBTs with the rated voltage of 3.3-kV are applied, 8 cells per leg and total of 96 units of IGBT are required. The number of cells and switching devices can be reduced compared with the case of 2.5-kV IGBTs. However, the switching frequency is limited because the switching speed is lower than the switching frequency of 2.5-kV IGBTs. Therefore, it is necessary to increase the value of DC capacitors since the response angular frequency of the control system is low.

In the case where IGBTs with the rated voltage of 6.5-kV are applied, 4 cells per leg and 48 units of IGBT are required. The number of cells and switching devices can be significantly reduced compared to 2.5-kV IGBTs and 3.3-kV IGBTs. The switching speed of 6.5-kV IGBT is lower than that of 2.5-kV IGBT and 3.3-kV IGBT. Furthermore, the large values of DC capacitor and buffer reactors are needed because angular frequency responses of the average control and the input current control become low, respectively. In addition, the large inductance of buffer reactors are also applied since the response angular frequency of the input current control becomes low. In the proposed system, MMC output is a high frequency voltage. However, the voltage drop becomes large since a voltage-dividing condition occurs between the high frequency transformer and buffer reactors. In the worst case, it is difficult to transmit a high frequency power to secondary side of the transformer when the buffer reactor is large. Therefore, it is necessary to reduce the inductance of buffer reactors to transmit the high frequency power.

Table 1. Parameters of switching devices and switching frequency.

	Device Parameters	f_s
2.5-kV IGBT IXBK64N250	V_{CE}=2.5 kV, I_c = 156 A E_{on} = 30.2 mJ @ Ic = 140 A, V_{CE} = 1.25kV, R_{Gon} = 1 Ω, V_{GE} = ±15 V E_{off} = 15.31 mJ @ Ic = 140 A, V_{CE} = 1.25kV, R_{Goff} = 1 Ω, V_{GE} = ±15 V V_{CEsat} = 2.5 V @ Ic = 64 A, V_{GE} = 15 V	5 kHz
2.5-kV_FWD SD203N/R25S20	V_{RRM}= 2.5 kV, I_c= 200 A V_{FM} = 1.65 V @ Ipk = 628 A	
3.3-kV_IGBT FF200R33KF2C	V_{CE}=3.3kV, I_c= 200A E_{on} = 235 mJ @ Ic = 200 A, V_{CE} = 1.8kV, R_{Gon} = 7.5 Ω, V_{GE} = ±15 V E_{off} = 215 mJ @ Ic = 200 A, V_{CE} = 1.8kV, R_{Goff} = 5.6 Ω, V_{GE} = ±15 V V_{CEsat} = 3.4 V @ Ic = 200 A, V_{GE} = 15 V	1.38 KHz
3.3-kV_FWD FF200R33KF2C	V_{RRM}= 3.3 kV, I_c= 200 A V_F = 2.8 V @ I_F = 200 A	
6.5-kV IGBT FZ400R65KE3	V_{CE}=6.5 kV, I_c=400 A E_{on} = 3450 mJ @ Ic = 400 A, V_{CE} = 3.6kV, R_{Gon} = 1.9 Ω, V_{GE} = ±15 V E_{off} = 2250 mJ @ Ic = 400 A, V_{CE} = 3.6kV, R_{Goff} = 13 Ω, V_{GE} = ±15 V	Under 1 kHz

Table 2. Comparison for numbers of cells and switching devices depending on the rated voltage of the switching device.

Rated Voltage	Numbers of Cells @leg	Numbers of Switching devices
2.5-kV	10	120
3.3-kV	8	96
6.5-kV	4	48

C. Evaluation of proposed system by appling SiC MOSFETs

SiC-MOSFET with the rated voltage of 10 kV has been developed [20]. SiC devices have following advantages: high rated voltage, low loss, high switching speed and high operating temperature. Therefore, Employing SiC devices to high power applications are

considered nowadays, especially, in the high voltage and high power conversion system. However, the dv/dt at winding wires of a high frequency transformer becomes greatly large. Thus, the insulation degradation among winding wires may occur when the proposed system is operated by using high rated voltage devices. From the previous topic, it is needed to set the switching frequency in order to modulate the operation frequency of the high frequency transformer at 1 kHz. Therefore, it is necessary to consider the operation of the proposed system when 3.3-kV SiC-MOSFET is applied into the proposed system. Note that the device data of 3.3-kV SiC-MOSFET was reported [21].

Table 3 shows the simulation parameters. The switching frequency of the SiC-MOSFET is set to 15 kHz. Note that the ideal elements are used in the switching device. In addition, the output voltage command is a square-wave of 2.3 kV, 1 kHz.

Fig. 3 shows the input phase voltage and current waveforms. From Fig. 3, it is confirmed that the unity power factor can be obtained in the input stage. Moreover, the total harmonic distortion (THD) of the input current is approximately 1.74%. The input current waveform includes few pulse beats. However, the pulse beats does not affect the THD of the input current since the frequency of the pulse beats is very high compared to the fundamental frequency.

Fig. 4 shows the output voltage waveform. From the result, the output voltage is constantly controlled approximately at 450 V. Moreover, the ripple voltage is obtained 0.4%. Thus, the power conversion from three-phase AC voltage into a DC voltage is confirmed.

Fig. 5 shows the cell capacitor voltage waveforms at the r-phase. The cell capacitor voltage is controlled according to the capacitor voltage command v_c^* by the average control and the balance control. In the capacitor voltage, the ripples include two frequency components: 100 Hz and 1 kHz. Then, the ripple of 1 kHz is less than that of 100 Hz. Furthermore, the ripple of 100 Hz comprises a majority of the capacitor voltage ripple. However, the maximum ripple of each capacitor voltage is obtained by 2.0%. Thus, it is confirmed that the voltage ripple does not affect the circuit operation in the proposed system.

Fig. 6 shows the output voltage waveforms of the MMC. It is confirmed that the high frequency AC voltage of 1 kHz is obtained. However, an error occurs between the output voltage of the MMC and the voltage command. The error depends on the voltage drop in each buffer reactor. Moreover, the output voltage waveform is dropped when the voltage polarity changes because the high frequency current flows in all diode in the rectifier circuit due to the leakage inductance condition of the high frequency transformer. The output voltage depends on the voltage drop of the leakage inductance.

D. Evaluation of total electrostatic energy

In general electrical products, the size of an electrolytic capacitor affects the system size. On the other hand, the size of a DC capacitor depends on the electrostatic energy because the size of the electrolytic capacitor depends on the charge voltage of the DC capacitor and its capacitance. Thus, the system size can

Table 3 Simulation condition

Output power P_O	400 kW	Input voltage rms	6.6 kV
Input voltage frequency	50 Hz	Output voltage	450 V
Number of cell per leg n	8	Load R	0.5 Ω
Turn ration pri.: sec.	1 : 1.5	Carrier frequency	15 kHz
Interconnection reactor L_{in}		4 mH ($\%Z$ = 1.15%)	
Buffer reactor L_b		0.5 mH ($\%Z$ = 0.31%)	
DC capacitor C		1,600 μF	
Output capacitor C_r		3,000 μF	
Switching device		3.3-kV SiC-MOSFET	

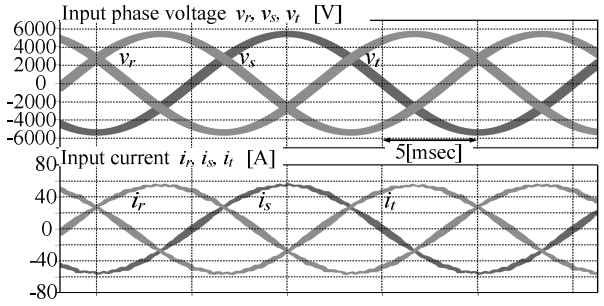

Fig. 3. Waveforms of the input phase voltage and current.

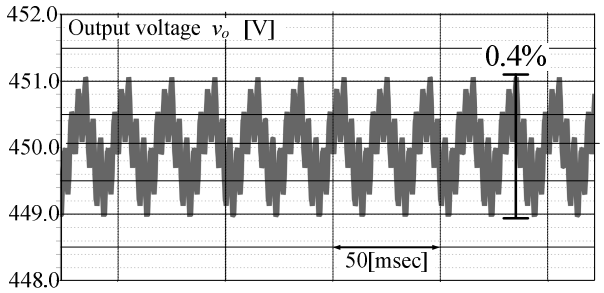

Fig. 4. Waveform of the output voltage at the diode bridge rectifier

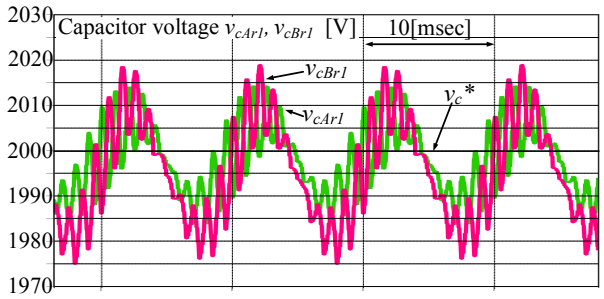

Fig. 5. Waveform of the capacitor voltage.

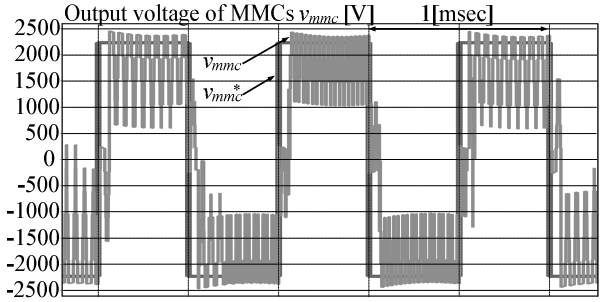

Fig. 6. Waveform of the MMC output voltage.

be evaluated by total electrostatic energy of the DC capacitor. The total electrostatic energy W_C is given by (5).

$$Wc = \frac{1}{2} C V_c^2 \times N \tag{5}$$

where C is a capacitance of each capacitor, N is the number of capacitors in MMC and V_C is the average value of the capacitor voltage. V_C is equal to the capacitor voltage command v_c^* when all capacitor voltage is kept constant by the average control and the balance controls.

On the other hand, the capacitance of the DC capacitor is designed in order to suppress the voltage ripple. At the DC capacitor, the ripple frequency of the voltage ripple becomes 100 Hz occurs because each cell rectifies the input current of the commercial frequency. In this paper, the capacitance of the DC capacitor is designed in order to suppress the voltage ripple of 100 Hz. Moreover, the ripple is suppressed within 1% against the average value of the capacitor voltage. Furthermore, it is necessary to set the capacitance of the DC capacitor to satisfy the requirement. In order to control the input current, the buffer reactor current i_a and the cell output voltage v_{sc} is given by (6).

$$\begin{aligned} i_a &= \frac{\sqrt{2}}{2} I \sin \omega t \\ v_{sc} &= 2\sqrt{\tfrac{2}{3}} E \sin \omega t \end{aligned} \tag{6}$$

where I is the effective value of the input current, E is the effective value of the input line voltage and ω is an angular frequency of the input voltage. Moreover, the current which flows to the DC capacitor is i_{dc}. The DC capacitor voltage v_c is kept at constant when $v_c i_{dc} = v_s i_a$ holds because input power and the output power are equal. From (6), the DC capacitor current i_{dc} is given by (7).

$$i_{dc} = \frac{EI}{\sqrt{3} v_c n} (1 - \cos 2\omega t) \tag{7}$$

The second term of (7) is the current ripple Δi_{dc}. In addition, the voltage ripple Δv_c can be calculated by the impedance of DC capacitor and the current ripple Δi_{dc}. From the relationship between the voltage ripple Δv_c and the capacitance of DC capacitor for the voltage ripple suppression is given by (8). Note that v_c is equal to the voltage command v_c^* in each system. From (8), the capacitance of each system can be calculated.

$$C = \frac{EI}{\sqrt{3} \Delta v_c n v_c^* \omega} \tag{8}$$

Fig. 7 shows the comparison result of the total energy which all capacitor charges. From the comparison result, the total electrostatic energy is the largest when 3.3-kV IGBTs are applied. In the case of applying 3.3-kV IGBTs, the capacitance should be larger than that is calculated by (8) since the response angular frequency of the average control becomes low.

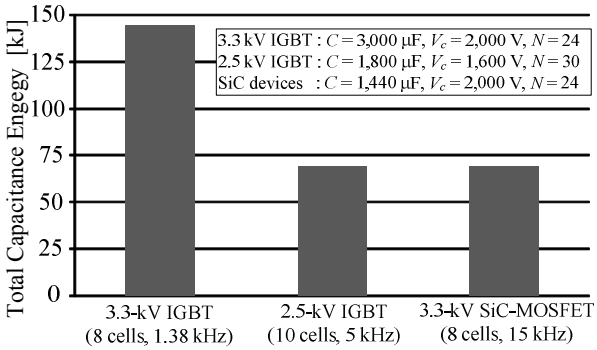

Fig. 7. Comparison of total electrostatic energy in DC capacitors

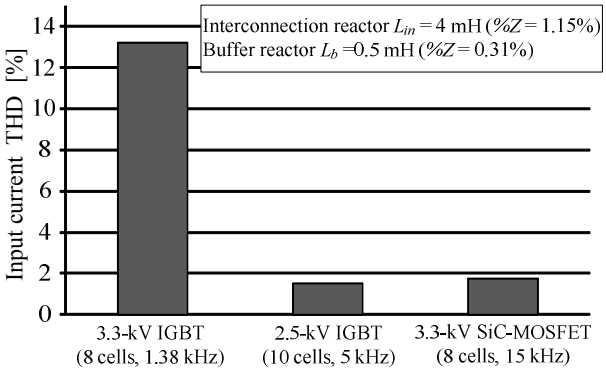

Fig. 8. Comparison of the input current THD according to the switching devices.

In the case of applying 3.3-kV SiC-MOSFETs into the proposed system, the total electrostatic energy is the lowest since the number of cells and the ripple voltage against the average value of the capacitor voltage are reduced. Furthermore, by applying 3.3-kV SiC-MOSFETs to the system, the size reduction of the proposed system can be achieved since the number of circuit components can be reduced and the power loss in switching devices can be suppressed.

In the case of applying 2.5-kV IGBTs into the proposed system, the total electrostatic energy is nearly identical to that of 3.3-kV SiC MOSFETs because the capacitance C and the capacitor voltage V_C become low. In conclusion, the size of DC capacitors can be reduced when 2.5-kV IGBTs are applied into the proposed system as well as 3.3-kV SiC MOSFETs.

E. Comparison with respect to THD of Input Current

Fig. 8 shows the comparison result of the input current THD. From Fig. 8, the THD is the lowest in the case where IGBTs with the rated voltage of 2.5 kV. When 2.5-kV IGBTs are applied into the proposed system, the number of cells is the highest. Furthermore, the harmonic distortion is suppressed because the input voltage becomes multilevel waveform due to multi-cells. On the other hand, when 3.3-kV SiC-MOSFETs are applied into the proposes system, the low THD of the input current is achieved as well as 2.5-kV IGBTs because it is possible to set a higher response angular frequency of the input current control due to the high switching speed. Finally, the THD is the highest in cases where IGBTs with the rated voltage of 3.3-kV. When 3.3-kV IGBTs are applied

into the proposed system, it is not possible to set a high response angular frequency because the switching speed of the IGBT is very low. Thus, it is difficult to improve the harmonic distortion for the system which is applied 2.5-kV IGBTs when the same values of the interconnection reactor and the buffer reactor are applied as well as the system which 2.5-kV IGBTs or 3.3-kV SiC-MOSFETs are applied.

F. Comparison Evaluation of the device loss

Fig. 9 shows the comparison result of the device losses: the conduction loss, the switching loss and the conduction loss of the FWD against the output power. Note that a SiC Junction Barrier Schottky Diode is applied as the FWD of 3.3-kV SiC-MOSFETs. Note that the device data of a SiC Junction Barrier Schottky Diode was reported [22].

In the case of applying 3.3-kV IGBTs to the proposed system, the switching loss is larger than the other system because turn-on loss and turn-off loss are large compared with the system which 2.5-kV IGBTs and 3.3-kV SiC-MOSFETs from Table 1. Moreover, the system using 3.3-kV IGBTs cannot achieve the efficiency of 95%. It is possible to achieve the efficiency of 95% when the low switching speed is set. However, the system cannot produce the high frequency output voltage when the low switching speed is set. In addition, in the system that is applied with low switching frequency devices, the value of the DC capacitor is needed to be increase in order to maintain the voltage of DC capacitors constantly.

In the case of applying 2.5-kV IGBTs, the efficiency of 95% can be achieved when the switching frequency is 5 kHz. Furthermore, it is possible to obtain the high frequency output voltage and keep the voltage of DC capacitors at constant. Moreover, when 2.5-kV IGBTs are applied into the proposed system, more cells are required rather than other systems. However, the system is able to achieve the efficiency of 95%. Thus, in the system which is applied 2.5-kV IGBTs, the number of cells is not significantly affected the efficiency.

In the case of applying 3.3-kV SiC-MOSFETs to the proposed system, the loss at switching devices is the lowest because both the turn-on loss and turn-off loss are lower than that of both IGBTs. Furthermore, the efficiency is the highest. Moreover, when the losses of the devices become half comparing to the system which is applied to 2.5-kV IGBTs at switching frequency of 5 kHz, the volume of the heat-sink can be dramatically reduced.

In conclusion, by applying 2.5-kV IGBTs or 3.3-kV SiC-MOSFETs, the high efficiency can be achieved in the proposed system. Moreover, SiC-MOSFET is the most suitable for the proposed system because SiC-MOSFET has the high performance features. Thus, the proposed system using 3.3-kV SiC-MOSFET reduces the harmonic distortion of the input current, can achieve the high efficiency and the size reduction of the system. On the other hand, 2.5-kV IGBTs also has good performance in terms of the efficiency and the suppression of the harmonic distortion.

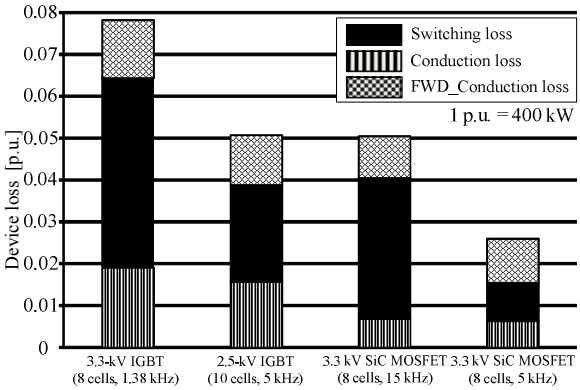

Fig. 9. Comparison of the switching loss and the conduction loss.

V. CONCLUSION

In this paper, an isolated three-phase AC-DC converter using MMC and the control strategy were proposed for a medium voltage application. The proposed system could directly convert an input three-phase voltage into a high frequency single-phase voltage. Therefore, the proposed system could reduce the volume of the isolated transformer since the single-phase high frequency transformer could be applied to the high frequency link.

The proposed system is evaluated with numbers of different rated voltage devices: a 2.5-kV IGBT, a 3.3-kV IGBT and a 3.3-kV SiC-MOSFETs. As a result, when 3.3-kV SiC-MOSFETs is applied into the proposed system, the total electrostatic energy in DC capacitors is the lowest compared to the other devices. Furthermore, 3.3-kV SiC-MOSFETs could achieve the size reduction of the proposed system when the common value of energy density in all capacitor is considered. Moreover, the system using 3.3-kV SiC-MOSFETs could achieve low THD input current waveform which is approximately 2.36% and the maximum ripple factor of each capacitor voltage is approximately 2.0%. Finally, from comparison evaluation of the efficiency when device losses are considered in the proposed system, it is confirmed that the efficiency of 95% can be achieved when 2.5-kV IGBTs and 3.3-kV SiC-MOSFET are applied into the proposed system. In conclusion, in the cases of 2.5-kV IGBTs and 3.3-kV SiC-MOSFETs, the proposed system can achieve the size reduction, the low THD of input current and high efficiency. Moreover, the system which is applied SiC-MOSFETs can achieve better efficiency compared with 2.5-kV IGBT even the same switching frequency is applied.

In future works, the optimized design method of the high frequency transformer for the high power application will be considered. In addition, the volume evaluation results of the proposed system compared to the conventional system will be shown.

REFERENCES

[1] E. Taylor , M. Korytowski and G. Reed ; “Voltage Transient Propagation in AC and DC Datacenter Distribution Architectures”,

Energy Conversion Congress and Exposition (ECCE), pp. 1998 - 2004, (2012)

[2] J. Lago and M. L. Heldwein ; "Operation and Control-Oriented Modeling of a Power Converter for Current Balancing and Stability Improvement of DC Active Distribution Networks", IEEE Trans. on Power Electronics, vol. 26, No. 3, pp. 877–885, (2011)

[3] Y. Morishita, T. Ishikawa, I. Yamaguchi, S. Okabe, G. Ueta and S. Yanabu ; "Applications of DC Breakers and Concepts for Superconducting Fault-Current Limiter for a DC Distribution Network", IEEE Trans. on Applied Superconductivity, vol. 19, No. 4, pp. 3658–3664, (2009)

[4] N. Hatti, K. Hasegawa and H. Akagi ; "A 6.6-kV Transformerless Motor Drive Using a Five-Level Diode-Clamped PWM Inverter for Energy Savings of Pumps and Blowers", IEEE Trans. on Power Electronics, vol. 24, No. 3, pp. 796–803, (2009)

[5] N. Hatti, Y. Kondo and H. Akagi ; "Five-Level Diode-Clamped PWM Converters", IEEE Trans. on Industry Applications, vol. 44, No. 4, pp. 1268–1276, (2008)

[6] P. K. Steimer and M. Winkelnkemper, "Transformerless Multi-Level Converter based Medium Voltage Drives", ECCE2011 pp. 3435 -3441, (2011)

[7] R.l Crosier, S. Wang and M. Jamshidi, "A 4800-V Grid-Connected Electric Vehicle Charging Station that Provides STACOM-APF Functions with A Bi-directional, Multi-level,Cascaded Converter", APEC2012, pp. 1508-1515R. Nicole, "Title of paper with only first word capitalized," J. Name Stand. Abbrev., in press.

[8] H. M. Pirouz and M. T. Bina, "New Transformerless STATCOM Topology for Compensating Unbalanced Medium-Voltage Loads", Power Electronics and Applications, 2009. EPE '09. 13th European Conference, (2009)

[9] H. Li, Thomas L. Baldwin, C. A. Luongo, and D. Zhang , "A Multilevel Power Conditioning System for Superconductive Magnetic Energy Storage", IEEE Trans. on Applied Superconductivity, Vol. 15, No. 2, pp. 1943-1946 (2005)

[10] F. Z. Peng, W. Qian and D. Cao ; "Recent Advances in Multilevel Converter/Inverter Topologies and Applications", Power Electronics Conference (IPEC), 2010 International, pp. 492-501 (2010)

[11] M. Glinka and R. Marquardt, "A new ac/ac multilevel converter family", IEEE Trans. Industrial Electronics, vol. 52, No. 3, pp. 662–669, (2005)

[12] M. Hagiwara and H. Akagi, "Control and Experiment of Pulsewidth-Modulated Modular Multilevel Converters", IEEE Trans. on Power Electronics, Vol. 24, No. 7, pp. 1737-1746 (2009)

[13] M. Hagiwara, R. Maeda and H. Akagi, "Negative-Sequence Reactive-Power Control by a PWM STATCOM Based on a Modular Multilevel Cascade Converter (MMCC-SDBC)", IEEE Trans. on Industry Applications, Vol. 48, No. 2, pp .720-729 (2012)

[14] M. Vasiladiotis, S Kenzelmann, N. Cherix and A. Rufer, "Power and DC Link Voltage Control Considerations for Indirect AC/AC Modular Multilevel Converters", Power Electronics and Applications (EPE 2011), Proceedings of the 2011-14th European Conference, (2011)

[15] Y. Hayashi, T. Takeshita, M. Muneshima and Y. Tadano ; "Independent control of input current and output voltage for Modular Matrix Converter", Industrial Electronics Society, IECON 2013 - 39th Annual Conference of the IEEE, pp. 888-893 (2013)

[16] H. Akagi and R. Kitada, "Control and Design of a Modular Multilevel Cascade BTB System Using Bidirectional Isolated DC/DC Converters", IEEE Trans. on Power Electronics, Vol. 26, No. 9, pp. 2457-2464 (2009)

[17] J. Shi, W. Gou, H. Yuan T. Zhao and A. Q. Huang ; "Research on Voltage and Power Balance Control for Cascaded Modular Solid-State Transformer", IEEE Trans. on Power Electronics, vol. 26, No. 4, pp. 1154–1166, (2011)

[18] S Kenzelmann, A. Rufer, M. Vasiladiotis, D. Dujic, F. Cnales and Y. R. de Novaes, "A versatile DC-DC converter for energy collection and distribution using the Modular Multilevel Converter", Power Electronics and Applications (EPE 2011), Proceedings of the 2011-14th European Conference, (2011)

[19] T. Nakanishi and J. Itoh, "Evaluation of control methods for isolated three-phase AC-DC converter using modular multilevel converter topology", ECCE-Asia Downunder pp. 52-58 (2009)

[20] J. Wang, T. Zhao, J. Li, A. Q. Huang, R. Callanan, F. Husna and A. Agarwal ; "Characterization, Modeling, and Application of 10-kV SiC MOSFET", IEEE Trans. on Electron Devices, Vol. 55, No. 8, pp. 1798-1806 (2008)

[21] R. Lai, L. Wang, J. Sabate, A, Elasser and L. Stevanovic, "High-Voltage High-Frequency Inverter using 3.3 kV SiC MOSFETs", Power Electronics and Motion Control Conference (EPE/PEMC), 2012, DS2b.6-1 - DS2b.6-5 (2012)

[22] T. Duong, A. Hefner, K. Hobart, S.H. Ryu, D. Grider, D. Berning, J. M. Ortiz-Rodriguez, E. Imhoff, J. Sherbondy, "Comparison of 4.5 kV SiC JBS and Si PiN Diodes for 4.5 kV Si IGBT Anti-parallel Diode Applications", Applied Power Electronics Conference and Exposition (APEC), 1057 - 1063 (2011)